Peer-reviewed version available at Molecules 2018, 23, 224; doi:10.3390/molecules23010224

Article

A Semi-Pilot Photocatalytic Rotating Reactor (RFR) with Supported TiO_2 /Ag Catalysts for Water Treatment

Carlos Montalvo[1], Claudia Aguilar [1,*], Roberto Alcocer[1], Miguel Ramirez[1]

[1] Department of Chemical Sciences, Universidad Autónoma del Carmen, Calle 56 No. 4, Avenida Concordia, CP 24180, Ciudad del Carmen, Campeche, México.

* Correspondence: alejandra175@hotmail.com

Abstract: A four stage semi-pilot scale RFR reactor with ceramic disks as support for TiO_2 modified with silver particles was developed for the removal of organic pollutants. The design presented in this article is an adaptation of the rotating biological reactors (RBR) and its coupling with the modified catalyst provides additional advantages to designs where a catalyst in suspension is used. The optimal parameter of rotation was 54 rpm and the submerged surface of the disks offer a total contact area of 387 M^2. The modified solid showed a decrease in the value of its bandgap compared to commercial titanium. The system has a semi-automatic operation with a maximum reaction time of 50 h. Photo-activity tests show high conversion rates at low concentrations. The results conform to the Langmuir heterogeneous catalysis model.

Keywords: rotating photocatalytic reactor; TiO_2 /Ag catalysts; water treatment

1. Introduction

Advanced oxidation processes (AOP) are widely used for water decontamination. Such processes rely on the photocatalysis principle, that is, the generation and use of the hydroxyl radical (·OH) in the presence of UV light with an adequate intensity. The photocatalytic process can reduce the initial organic matter to CO_2, H_2O and mineral salts. This technology has proved its efficiency for the complete elimination of different organic molecules. The basic principles have been widely reported in the literature [1-3]. However, one of the processes that decreases the efficiency of the photocatalytic process is the recombination of charges since it generates neutral centers. To prevent this, the reaction medium can be added with an element such as oxygen, which sequesters the electron from the valence band or metallic nanoparticles.

Photocatalysis is an efficient treatment of drug degradation [4], as well as chlorinated organic compounds, nitrogenous compounds, aromatic hydrocarbons such as trichlorethylene, chloroform, chlorophenols. [5] The emergence of so-called "emerging pollutants" (drugs, pesticides, Personal hygiene products) creates an additional problem due to the scarce information available on its effects on the environment or its interference with biological processes [6].

This work shows water treatment with photocatalytic processes and their coupling to the RFR (Rotating Photocatalytic Reactor). This type of reactor manages to reduce some of the main challenges of the photocatalysis, such as the use of the catalyst in suspension. Its design is part of the biological contactors and can be used as a hybrid reactor. The treatment capacity of this design is 50 L, so it can be considered a viable option to treat small volumes of industrial water.

1.1 The rotating photocatalytic reactor (RFR)

There are important factors to consider when designing a photocatalytic reactor. The need to use a solid catalyst complicates the process by adding another phase to the system. In this type of reactors, it becomes evident that, besides making the contact between the reagents and the catalyst (high catalyst surface area per unit volume of the reactor) efficient, a high exposure of the catalyst to the

radiation (optimal distribution of light inside the equipment) is required. A photo-reactor of rotating disks, considered a novel photo-reactive system and suitable for large scale applications, is a good example of a system that uses the supported photocatalyst and can operate with sunlight or UV light in a continuous system. RFR arise as an adaptation of rotating biological reactors (RBR), while retaining the following advantages:

A) Low energy consumption

B) Simplicity of operation and maintenance

C) Minimization of space and volume required

D) Simplicity in assembly

One of the first works to explore the benefits of these designs was done by Dionysios et al. [7]. The research shows that the initial increase in reaction velocity with respect to the angular velocity of the disk is attributed to the time available per rotation. The rate of decomposition of 4-chlorobenzoic acid showed Langmuir-Hinshelwood kinetics. The results obtained suggest the absence of significant mass transfer limitations at angular velocities greater than 6 rpm.

For inactivation of bacteria *Escherichia coli* [8]; the use of this type of reactor showed its best behavior after varying parameters such as the speed of rotation of the disks, the intensity of radiation and the number of disks. There are few current references and developments for RFR. Recent developments are concentrated in few papers published in recent years, Zhan et al. [9] combined a system of titanium oxide nanotubes in a rotary disk reactor (RDPR) performing degradation tests with rhodamine B. The conversion rates were greater than 90% after a three-hour reaction. While these works only show the coupling of different forms and modification of the catalysts in a photo-catalytic system, the contributions made by these have led to improvement and a better understanding of the photocatalytic phenomena.

Nan Lin et al. [10] designed a photo-catalytic rotary disks reactor (MLRDR). The catalyst was immobilized on the disks by multilayers. The main contributions of this work are focused on the influence of the number of layers and the volumetric flow velocity. Nan Lin concluded that the efficiency of the reactor relies completely on these parameter. The diameter of the disks used in this design was 12 cm.

Cheng Yang et al. [11] developed a study based on a well-developed photocatalytic fuel cell equipped with dual rotating disks for wastewater treatment. The innovation in this new device was the use of a hemoglobin on graphite cathode for in situ hydrogen peroxide (H_2O_2) generation. This design uses the invalid excited electron from the photoanode and enhances the overall performance of Rhodamine B degradation compared with the cells using the cathode without Hb. Compared to traditional photocatalytic reactors, this photocatalytic fuel cell shows greater better utilization efficiency of incident light and a higher degradation performance of organic pollutants.

Recently Li et al. [12] developed a system of rotary disks for post-treatment of water in the textile industry. The main contributions of this work is in the structure of the disks since they exhibit a high surface and an efficient use of UV light. The operating conditions of the disks were 20 rpm and the initial capacity of the reactor was 120 mL.

Fang Li et al. [13], showed other advances in the development of the PRD reactor (Photocatalytic rotating disks) by adding H_2O_2 to increase the mineralization of the orange methyl dye. The main contribution of this design is an improved capacity of treatment of 5 L.

1.2 Modification of catalysts

Photocatalysis has been proved to be an efficient process for the removal of different organic molecules, but a major drawback is the "recombination of charges" since it decreases the efficiency of the process. In this scenario, the doping of catalysts is an efficient way to achieve deposition of metallic ions in the surface of the catalyst to change its electrical properties and increase its efficiency for photocatalytic processes. TiO_2 is an excellent support because its structure consists of small particles of nano-metric size with a large surface area in which metallic silver can be deposited to

avoid the recombination process. It also allows the availability of photo-generated holes for the reaction [14]. The deposition of Ag in TiO_2 confers anti-bacterial capacity, making it an efficient material for virus inactivation in water treatment [15]. Likewise the wavelength of catalysts modified with nano-metallic particles can be extended to visible light [16-17]. The effect of silver-doped titanium irradiated with UV light improves photocatalytic activity and improves separation of the electron-hole pair [18].

2. Materials and methods

2.1. Synthesis and coupling of the catalyst TiO_2 / Ag to the RFR

For the photo-deposition process, $AgNO_3$ precursor salts were used. The mass used was estimated based on a weight / weight ratio. Initially the solution containing the catalyst remained for one hour in the dark phase, then it irradiated by four 365 nm lamps for 2 h with the addition of nitrogen (80 cm ^{3}/ min). Water is removed by vacuum filtration, the material is dried at a temperature of 100 ° C and calcined at 550 ° C. The particle size was homogenized and impregnated in wet ceramic disks with a ratio of 2 g / M^2. The area covered by the discs was 3.5185 M^2 representing a contact area of 387 M^2 / gr available for the reaction. Finally the impregnated disks were calcined at a temperature of 550° C.

2.2 Characterization of the catalyst

The surface morphological analysis by secondary electrons and chemical analysis by energy dispersive spectroscopy (EDS) was performed in a Dual Beam Scanning Electron Microscope (FIB / SEM) FEI-Helios Nanolab 600 from the National Laboratory of Nanosciences and Nanotechnology Research (LINAN). XRD analyses were performed with a Rigaku, SMART LAB model using a copper tube as the X-ray source. The estimation of the band gap value (*Eg*) was performed by UV spectroscopy using a Shimadzu UV-2450 equipment, provided with the ISR-2200 Integrating Sphere Attachment.

2.3 Photoactivity tests

The photoactivity tests were performed with solutions of acetaminophen at different concentrations. For analysis of reaction kinetics samples were taken at different time intervals which were filtered with a Millipore GV membrane (pore diameter 0.22 μm). The final solution was analyzed using High Performance Liquid Chromatography (HPLC) on an Agilent 1100 Series equipment with the following specifications: Column Zorbax ODS 4.6 x 150 mm, 5 µm; flow conditions: 1 mL / min, Detector: UV-vis at 242 nm; Mobile phase: water-methanol (50/50).

3. Results

3.1 Characteristics of RFR

The configuration and dimension of RFRs provides a high area of contact between the solid and aqueous phase; in this system the catalyst is supported on ceramic disks. The contact between disks and aqueous phase form thin films of water on the disks; one phase is in contact with water and the other with air; the water adhering to the disk comes into contact with both the oxygen in the atmosphere and with the ultraviolet light or natural light that is irradiated by the lamps. In this design, 40% of the disks area is submerged.

The main characteristics of the Rotary Photocatalytic Reactors (RFR) are described in Table 1 and Table 2. The RFR is provided with a storage tank with a capacity of 50 L that are periodically supplied to the reaction system and has a control of the speed of rotation. Its operation allows to maintain conditions continuously and its design allows to take samples of the progress of the reaction in each of the stages without stopping the operation of the system. An RFR scheme is shown in Figure 1.

Peer-reviewed version available at Molecules 2018, 23, 224; doi:10.3390/molecules23010224

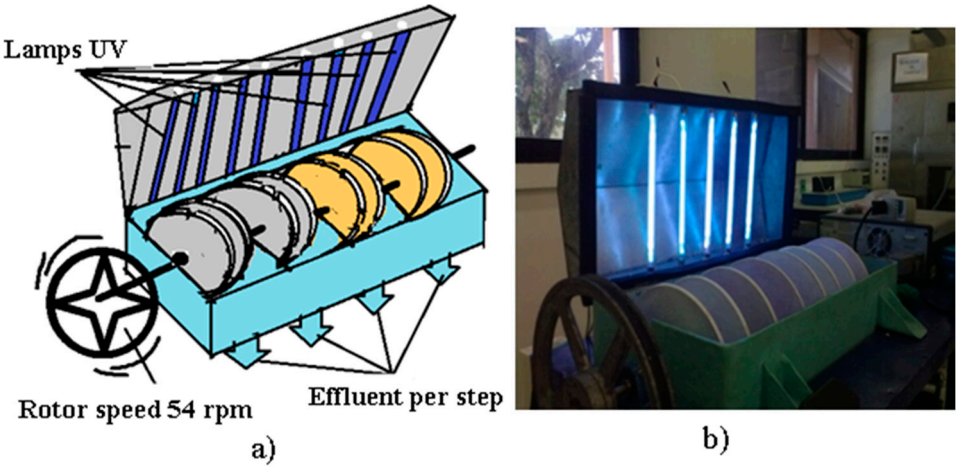

Figure 1. a) Schematic of the operation of the RFR adapted with UV lamps of λ = 254 nm, rotation speed= 54 rpm, the RFR has eight disks impregnated with TiO_2-Ag catalyst. b) Image of RFR in operation

Table 1. RFR design features

Characteristics of the disks	
Number of stages	4
Number of disks for stage	2
Material	ceramic
Diameter	0.24 m
Thickness	0.006 m
Area per stage	0.09047808 cm^2
Total area	0.36191232 cm^2

Table 2. RFR reactor operating characteristics

Parameter	**Characteristics**
Structure	Semi-cylindrical cover of stainless steel
Number of lamps	6 UV lamps (254 nm) oriented perpendicular to the reactor
Disks	Assembled on one axis (stainless steel, diameter: 0.25 inches, length = 70cm)
Volume (L)	3 L for each stage
Catalyst	TiO_2 doped with silver (5%)
Optimum rotation speed	54 rpm

3.1 Characterization of the catalyst (XRD, EDS and Diffuse reflectance)

The diffractogram of the catalyst is shown in figure 2. Differences are observed with respect to the titanium oxide without doping (Degussa P-25), intensities in 2θ = 45, 65 corresponding to metallic silver. There is no significant variation of the percentages of anatase with respect to the P-25. There are evident peaks that show the presence of silver indicating the distribution of the particles in the catalyst. The results are consistent with other studies where [19] defined peaks for Ag / TiO_2 have been determined in 38.2, 44.4 and 64.5.

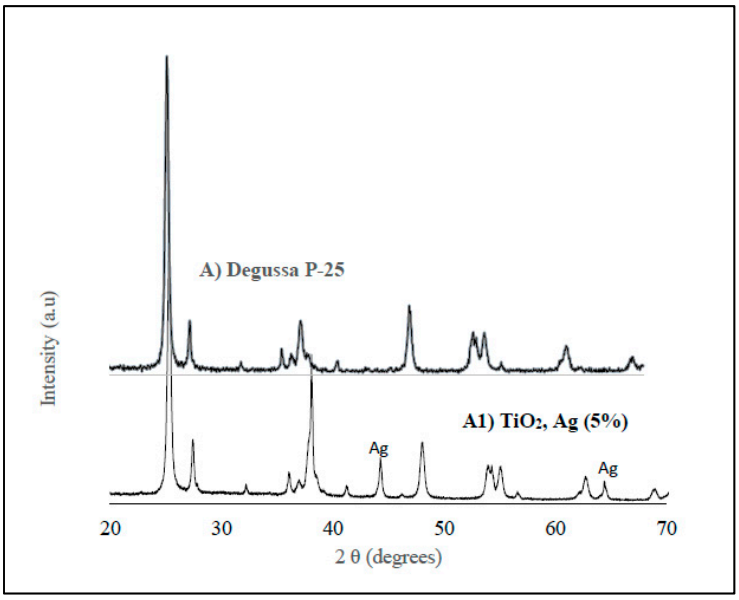

Figure 2. X-ray diffraction pattern of the silver nanoparticle-modified catalyst (A1) compared to the commercial catalyst (A). Different intensities are shown to the commercial catalyst that are attributed to the metallic silver.

Elemental analysis of the catalyst (figure 3) was performed using energy dispersion spectroscopy (EDS). During the calcination, the dispersed ions of Ag + gradually migrate to the TiO_2 surface and are deposited by improving the photocatalytic activity [20].

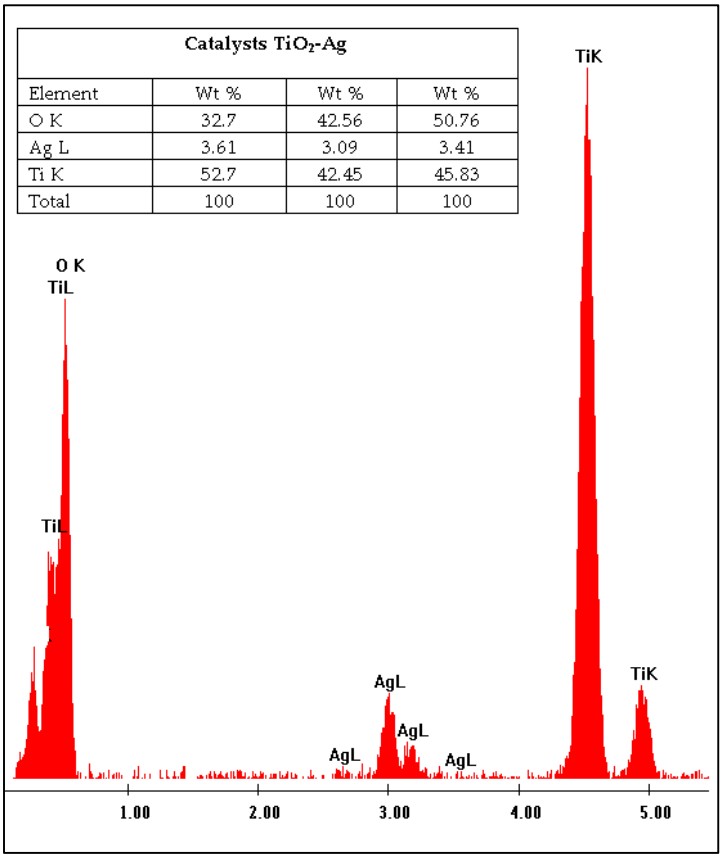

Catalysts TiO_2-Ag			
Element	Wt %	Wt %	Wt %
O K	32.7	42.56	50.76
Ag L	3.61	3.09	3.41
Ti K	52.7	42.45	45.83
Total	100	100	100

Figure 3. Elemental analysis of catalyst showing fractions of titanium, oxygen and silver metal. The results of three measurements made on the catalyst are shown. The average weight of the metallic silver deposited is 3.3%, the theoretical percentage was 5%.

Figure 4 shows the changes in the properties of the titanium surface by the presence of silver nanoparticles. There is an increase in the absorption due to resonance of plasmons in the surface between 500 and 600 nm. The efficiency of the catalysts with nano-silver particles can modify the levels of fermi energy which is displaced near the bottom of the conduction band causing the accumulation of electrons to influence the band of uptake of plasmons [21]. This can improve the photocatalytic activity of the material in the visible region. For the band gap calculation the function of the Kubelka Munk was transformed by interpreting the diffuse reflectance spectrum. The wavelength data is converted to frequency by the relation:

$$v = \frac{c}{\lambda_g} \quad (1).$$

$(Abs * hv)^{\frac{1}{2}}$ is plotted as a function of hv and a line is extrapolated to the X axis, which generates the estimated value of the band gap.

$$E_g = \frac{hc}{\lambda_g} = \frac{h(v\lambda_g)}{\lambda_g} = hv \quad (2)$$

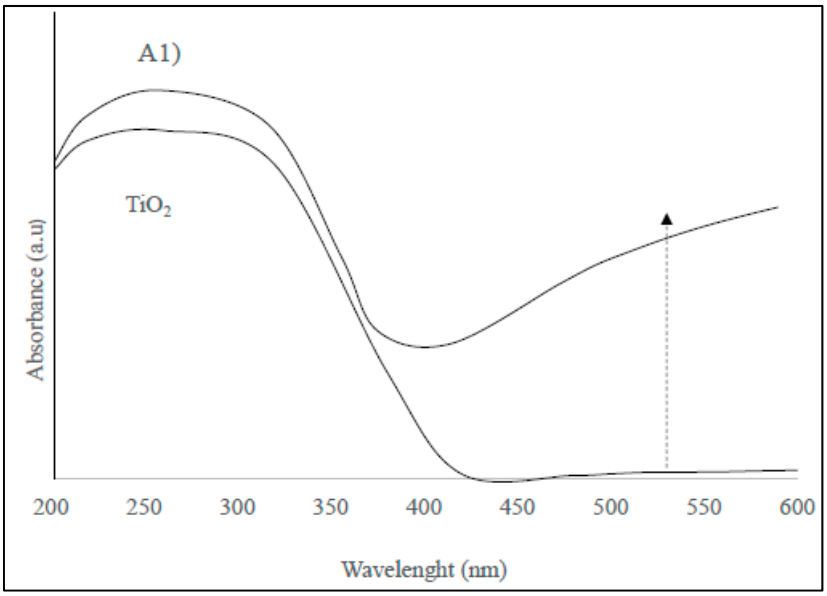

Figure 4. Comparison of the diffuse reflactance spectrum of the commercial catalyst TiO_2 with the catalyst modified with nano-silver particles. The absorption of the material (A1) in the visible light range is shown around 500 nm

3.2 Kinetics of the reaction

The optimum rotation speed was 54 rpm. The conversion factor of acetaminophen (30 mg / L) to these conditions was 73% achieved by raising the contact between the aqueous and solid phases, The efficiency of the system was determined by the acetaminophen photo-activity tests at concentrations of 20-160 mg / L with the purpose of knowing the effect of the concentration of the substrate on the rate of degradation. Thus, in all tests samples were taken to determine the degree of progress of the reaction. The samples were filtered and analyzed by Agilent 1100 Series High Performance Liquid Chromatography (HPLC) Column: Zorbax ODS 4.6 x 150 mm, 5 µm, flow conditions: 1 mL / min Detector: UV-vis at 242 nm, Mobile phase: 50/50 water-methanol. The results were also evaluated by UV-vis spectroscopy using an Agilent Cary 60.

The percentage of removal was calculated with the relation:

$$\%DEG = \left(1 - \frac{C_{TF}}{C_0}\right) x100 \quad (2)$$

Where: CTF = is the final concentration determined by liquid chromatography and C_0 = initial concentration.

Figure 5 shows the conversion rates obtained by varying the reactant concentration, rotational speed of the discs and the amount of light received.

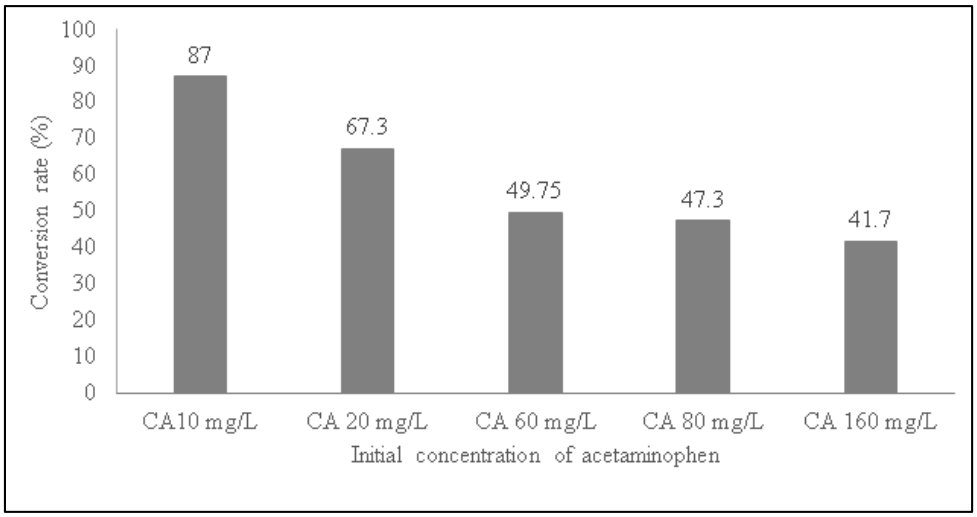

Figure 5. Percentages of conversion of the degradation of acetaminophen to different concentrations (catalyst mass = 1gr / L, rotational speed = 54 rpm, radiation of λ = 254 nm, number of lamps = 6, reaction volume= 12 L, Maximum reaction time = 50 hr)

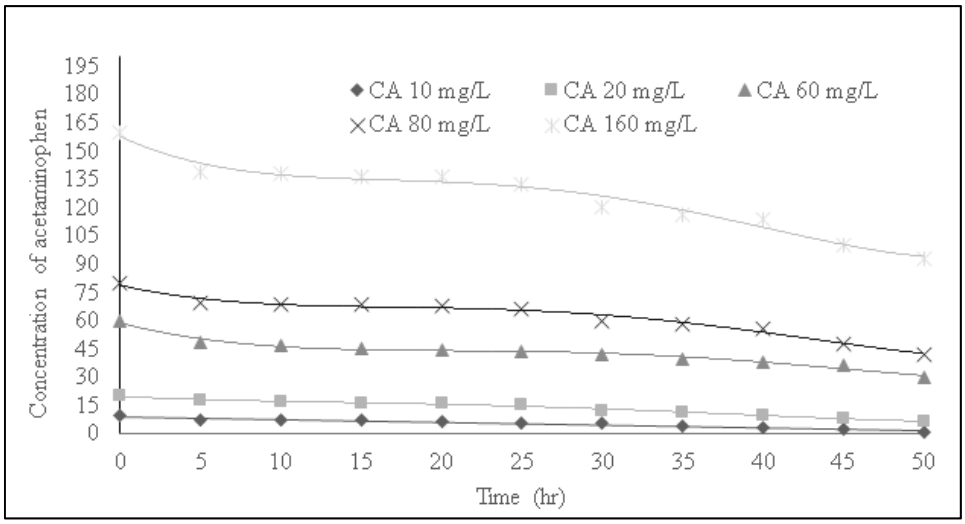

Figure 6. Profile of the degradation of acetaminophen followed by HPLC (catalyst mass = 1gr / L, rotational speed = 54 rpm, radiation of λ = 254 nm, number of lamps = 6, reaction volume= 12 L, Maximum reaction time = 50 hr)

The initial concentration is of paramount importance in the photocatalytic reactions since there is a high dependence of the concentration on reactions analyzed under the behavior of the first order kinetics [22]. The experimental data were analyzed under the concept of LH equation for heterogeneous catalysis checking the effect of the initial concentration on the reaction rate; (equation 3,4)

$$-r_{AC} = -\frac{dC_{AC}}{dt} = \frac{K_1 C_{AC}}{1 + K_2 C_{AC}} \quad (3)$$

$$-r_{AC} = \frac{0.024715 C_{AC}}{1 + 0.02878 C_{AC}} \quad (4)$$

The values of the kinetic constants K_1 = 0.0247157 $(min)^{-1}$ and K_2 = 0.02878 $(mg / L)^{-1}$ were obtained by nonlinear regression using the Levengerd Marquart algorithm. The experimental data was fitted to the LH catalytic model as shown in Figure 7.

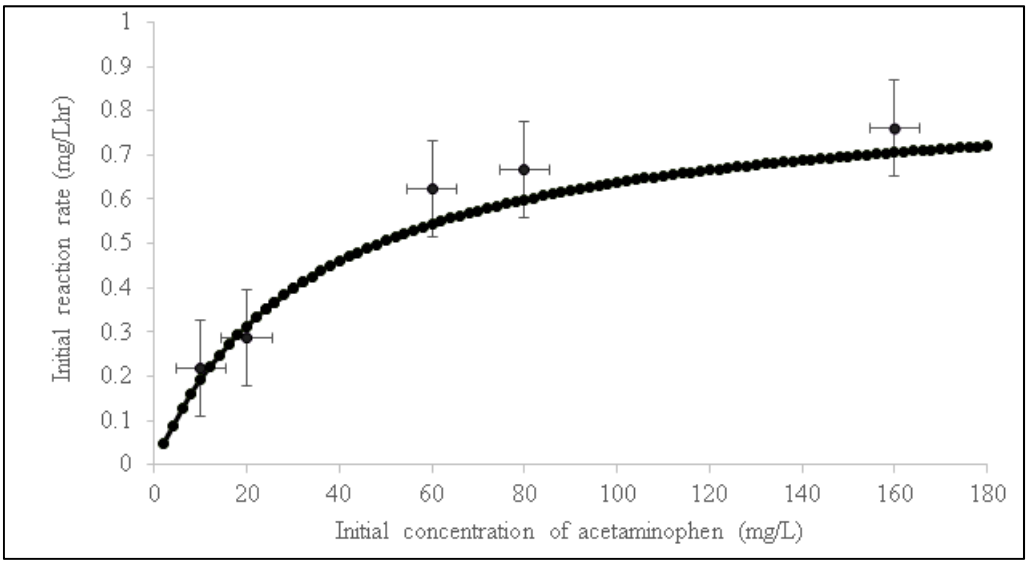

Figure 6. Heterogeneous LH catalysis model applied to the degradation of acetaminophen in an RFR reactor. The solid line represents the model and the points represent experimental data (catalyst mass = 1gr / L, rotational speed = 54 rpm, radiation of λ = 254 nm, number of lamps = 6, reaction volume= 12 L, Maximum reaction time = 50 hours)

5. Conclusions

In this article, a current development is shown for the design of the photocatalytic reactors with the use of a supporting catalyst modified with silver nano-particles. The method of preparation of the modified catalyst proved to be efficient after silver nanoparticles were added to their surface. A major advantage was the reduction of the bandwidth of the catalyst which may be potentially used with visible light.. The conversion rates can be as high as 87% in a maximum time of 50 h. Currently, there are no similar developments on the semi-pilot scale which incorporate automated processes.

Another advantage is the volume to be treated. Working volumes can be up to 40 L and can be operated continuously or by batch. The contact area provided by the four stage semi-pilot scale RFR reactor surpasses current reactors and it is adaptable to small spaces. The results obtained place it as a feasible option if implemented on a larger scale.

The influence of nano-silver catalyst particles on microbial activity, the use of visible light and the inclusion of controlled dosing of H_2O_2 to reduce hydraulic residence times will be objects of study in the future.

Acknowledgments: To the National Council of Science and Technology of Mexico (CONACYT) for the financing of project 169404.

Author Contributions: Montalvo C., designed the reactor as well as the coupling with modified catalysts, Aguilar C., synthesized the catalysts and Alcocer R., performed the photoactivity tests. Ramírez M., collaborated in the writing of the manuscript

Conflicts of interest: the authors declare no conflicts of interest

References

1. Lacombe, S.; Keller, N. Photocatalysis: fundamentals and applications in JEP 2011. *Environ. Sci. Pollut. Res.* 2012, 19, 3651–3654..
2. Kazuya, N.; Fujishima, A. TiO_2 photocatalysis: Design and applications. *J. Photochem. Photobiol. C: Photochemistry Reviews.* 2012,13, 169–189
3. Maeda, K. Photocatalytic water splitting using semiconductor particles: his tory and recent developments, *J. Photochem. Photobiol. C.* 2011, 12,237–268.
4. Yang, L.; Yu, L.; Ray, M. Photocatalytic oxidation of paracetamol: dominant reactants, intermediates, and reaction mechanisms. *Environ. Sci. Technol.*2009, 43 (2), 460-465.
5. Bolog, N.; Ismail, A.F.; Salim, M.R.; Matsuura, T. Review of the effects of emerging contaminants in wastewater and options for their removal. *Desalination* 2009, 239, 229–246.
6. Migowska, N.; Caban M.; Stepnowski, P.; Kumirska, J. Simultaneous analysis of non-steroidal anti-in flammatory drugs and estrogenic hormones in water and wastewater samples using gas chromatography mass spectrometry and gas chromatography with electron capture detection. *Science of the Total Environment.* 2012, 441, 77-88
7. Dionysiou, D.T.; Suidan, M.; Baudin, I.; Lainé, J.M. Oxidation of organic contaminants in a rotating disk photocatalytic reactor: reaction kinetics in the liquid phase and the role of mass transfer based on the dimensionless Damköhler number. *Applied Catalysis B: Environmental*. 2002,38, 1-16.
8. Hincapié, J.M.; Marín, J.M.; Ríos, L. A.; Restrepo G. Evaluación de la degradación de E. coli empleando un fotorreactor de discos rotatorios. *Revista Ingeniería e Investigación*.2007, 27, 65-69.
9. Zhang, A.; Zhou, M.; Han L.; Zhou, Q. The combinating of rotating disk photocatalytic reactor and TiO_2 nanotube arrays for the environmental pollutants removal. *Journal of Hazardous Materials.*2011, 186, 1374-1383.
10. Lin, C. N.; Chang, C. Y.; Huang, H. J.; Tsai, D. P.; Wu, N. L. Photocatalytic degradation of methyl orange by a multi layer rotating disk reactor. *Environmental Science and Pollution Research.*2012. 19, 3743-3750
11. Chen, Y.; Yi, H.; Diwen, Y.; Ye, Y.; Tiantian, T.; Yaling, W.; Jinping J. Ahigly efficient dual rotating disk photocatalytic fuel cell with wedged surface TiO_2 nanopore anode and hemoglobin cathode. *Catalysts* 2016, 6, 2-12.
12. Li, K.; Zhang, H.; He, Y.; Tang, T.; Ying, D.; Wang, Y.; Sun, T.; Jia, J. Novel wedge structured rotating disk photocatalytic reactor for post treatment of actual textile wasterwater. *Chemical Engineering Journal*. 2015,268, 10-20.
13. Fang, L.; Wai, S.; Haibao, H.; Jiantao, L.; Leung, Y.C. A photocatalytic rotating disc reactor with TiO_2 nanowire arrays deposited for industrial wasterwater treatment. *Molecules*.2017, 22, 2-13
14. Hinstho, N.; Petrik, L.; Nechaev, A.; Titinchi, S.; Ndungu, P. Photocatalytic activity of titanium dioxide carbon nanotube composites modified with silver and palladium nanoparticles. *Applied Catalysis B: Environmental.* 2014, 156, 273-283.
15. Hong, W.W.; Hsiu, C.L.; Chien, H.K.; Yue, L.C.; Yun, C.Y. Synthesis and photocatalysis of mesoporous anatase TiO_2 powders incorporated Ag nanoparticles *J. Phys. Chem. Solids*.2008, 69, 633–636
16. Jacob, M.; Levanon, H.; Kamat, P.V. Charge Distribution between UV-Irradiated TiO_2 and Gold Nanoparticles: Determination of Shift in the Fermi Level. *Nanoletters* 2003, 3, 353-358
17. László, A.; Kőrösi, L.; Papp, S.; Ménesi, J.; Illés , E.; Zöllmer, V.; Richardt, A.; Dékány, I. Photocatalytic activity of silver-modified titanium dioxide at solid–liquid and solid–gas interfaces. *Colloids and Surfaces A: Physicochem. Eng. Aspects.* 2008, 319,136-142.
18. Liga, M.V.; Bryant, E.L.; Colvin, V.L.; Li, Q. Virus inactivation by silver doped titanium dioxide nanoparticles for drinking water treatment. *Wat. Res.* 2011,45, 535-544
19. Serry, M.K.; Reenamole, G.; Floris, P.; Pillai, S.C. Silver doped titanium dioxide nanomaterials for enhanced visible light photocatalysis. *J Photochem Photobiol A: Chem.* 2007, 189:258-263
20. Liiev, V.; Tomova, D.; Bilyarska, L.; Eliyas, A.; Petrov, L. (2006) Photocatalytic properties of TiO_2 modified with platinum and silver nanoparticles in the degradation of oxalic acid in aqueous solution *Applied Catalysis B:Environmental*. 2006, 63,266-271.
21. Tran, H.; Scott, J.; Chiang, K.; Amal, A. Clarifying the role of silver deposits on titania for the potocatalytic mineralization of organic compounds. *Journal of photochemistry and Photobiology A: Chemistry*.2006, 183, 41-52.

290 22. Aguilar, C.; Montalvo, C.; Ceron, J.; Moctezuma, E. Photocatalytic degradation of acetaminophen. *Int. J.*
291 *Environ. Res*. 2011, 5(4), 1071-1078